Tom Schroeter

The Cinola Gold Deposit, Queen Charlotte Islands, British Columbia

N. CHAMPIGNY and A.J. SINCLAIR
Department of Geological Sciences
University of British Columbia
Vancouver, B.C.

ABSTRACT

The Cinola gold deposit in the northern Queen Charlotte Islands, British Columbia, is in a clastic sequence consisting of a lower shale of the Late Cretaceous Haida Formation and an overlying interbedded sequence of pebble conglomerate and coarse-grained sandstone of the Middle Miocene Skonun Formation. Both formations are intruded by a stock and dykes of porphyritic rhyolite. Two K-Ar model ages indicate mineralization and probably porphyritic-rhyolite intrusion at about 14 Ma (middle Miocene). A splay of the Sandspit fault system constitutes the footwall on the west of the deposit.

The Cinola deposit can be classed as Carlin-type based on features such as (1) small particle size for gold, (2) Tertiary age of mineralization, (3) element abundances (e.g. high Hg), (4) dominantly argillic alteration, (5) a structural setting associated with major faults, (6) porosity of the host rock and (7) spatial and possibly genetic association with felsic intrusions. Gold is widespread and occurs mainly as grains of < 0.5 µm in silicified sedimentary rock, and in quartz veins. Locally, coarse > 100 µm particles of native gold occur in quartz veins, especially in strongly brecciated porphyritic-rhyolite. Ore minerals are mainly pyrite and marcasite, but include small amounts of chalcopyrite, sphalerite, galena, pyrrhotite, cinnabar, tiemannite (HgSe), rutile, magnetite, hematite and limonite in addition to native gold and electrum. No silver minerals have been found; silver was found in gold particles in amounts varying from 6.2 to 24.2 weight per cent. Alteration products are sericite, illite, kaolinite and chlorite, with abundant quartz of several stages.

The host rocks, specifically the Skonun Formation, formed as an alluvial plain facies in a braided river system discharging into a marine basin in early Middle Miocene time. During the Middle Miocene, this sequence was intruded by a rhyolitic stock. The highly porous and permeable Miocene clastic sequence apparently provided an optimum setting for the development of a large geothermal system, the energy for which probably derived from the rhyolite stock. Mineral deposition followed a well-defined paragenesis, which, from oldest to youngest, is: (1) precipitation of iron sulphide minerals, and early quartz; (2) several stages of quartz veins, with deposition of sphalerite succeeded by galena, chalcopyrite and visible gold. Micron-size gold was precipitated throughout these two stages of mineral deposition. Argillitization of the host rocks probably in part coincided with the mineralization and continued during cooling of the geothermal cell.

In-situ reserves have been estimated at 41.1 million metric tons averaging 1.85 g Au/tonne using a cutoff grade of 0.86 g Au/tonne.

RÉSUMÉ

Le gisement Cinola (Specogna) est localisé dans une séquence de mudstones (Formation Haida, Crétacé supérieur) et une séquence de conglomerats à cailloux interlites avec des grès grossiers (Formation Skonun, Miocène Moyen). Un stock de rhyolite porphyrique fait intrusion à travers les deux séquences. Deux datations par la méthode potassium-argon indiquent un âge d'intrusion et de minéralisation d'environ 14 Ma. (Miocène Moyen). Une faille parallele à la faille régionale Sandspit constiue l'éponte ouest du gisement et marque un contact abrupte avec la séquence de mudstones.

Le gisement Cinola peut être classifie du type Carlin suivant les critères communs suivants: (1) petite taille des particules d'or, (2) âge de la minéralisation (Tertiaire), (3) géochimie (anomalie en mercure par exemple), (4) altération (surtout argillique), (5) contexte structural (association des failles majeures), (6) porosité des roches hôtes, (7) association spatiale et génétique avec des intrusions felsiques. La minéralisation aurifère est étendue et consiste en des particules submicroscopiques (< 0.5 µm) dans les sédiments silicifiés, et dans les veines de quartz. Localement, des grains grossiers (> 100 µm) d'or sont observés dans les veines de quartz, spécialement dans les rhyolites porphyriques brèchiques. Les minéraux opaques observés sont presqu'éxclusivement la pyrite et la marcasite. De faibles quantités de chalcopyrite, sphalerite, galène, pyrrhotite, cinnabar, tiemannite (HgSe), rutile, magnetite, hématite et limonite sont aussi presentes en plus de l'or natif et de l'électrum. Aucun minéral d'argent a été identifié; de l'argent est contenu dans les particules d'or dans des proportions qui varient de 6.2 a 76.4 pourcentage poids. Les minéraux d'altération sont la séricite, l'illite, la kaolinite, et la chlorite. Le quartz épithermal est très abondant.

Les sédiments mineralisés d'age Miocène Moyen ont été déposés par un fleuve possédant un drainage tresse qui se déchargeait dans un bassin marin. L'intrusion du stock de rhyolite porphyrique au Miocène Moyen a créé une immense cellule géothermale, l'énergie de celle-ci étant derivée de l'intrusif.

La minéralisation aurifère s'est produite suivant la paragenèse suivante (du plus vieux au plus jeune): (1) précipitation des sulfures de fer et d'une première génération de quartz, (2) plusieurs épisodes de veines de quartz accompagnés par la deposition de la sphalerite suivie par la galène, la chalcopyrite et l'or visible. L'altération de type argillique a probablement debuté pendant la minéralisation et s'est continuée durant le refroidissement de la cellule géothermale. Le minerai prouvé a été estimé a 45.4 millions de tonnes avec une teneur moyen en or de .054 once Au/tonne courte en utilisant une teneur de coupure de .025 once Au/tonne courte.

Introduction

The Cinola gold deposit, known also as the Babe and Specogna deposit, is central to Graham Island, the northern of the two largest Queen Charlotte Islands (Figure 1). It is accessible by about 18 km of logging road south from the town of Port Clements. Five companies optioned the property successively from 1971 to 1975 (Champigny *et al.*, 1980). Consolidated Cinola Mines Ltd. acquired the claims by option in 1977 and purchased them in 1978. Since August 1979, Energy Reserves Group and Consolidated Cinola Mines Limited have undertaken a 50-50% joint evaluation venture on the property. Indicated open-pit reserves are estimated at 41.1 million metric tonnes grading 1.85 g Au/tonne, using a cutoff of 0.86 g

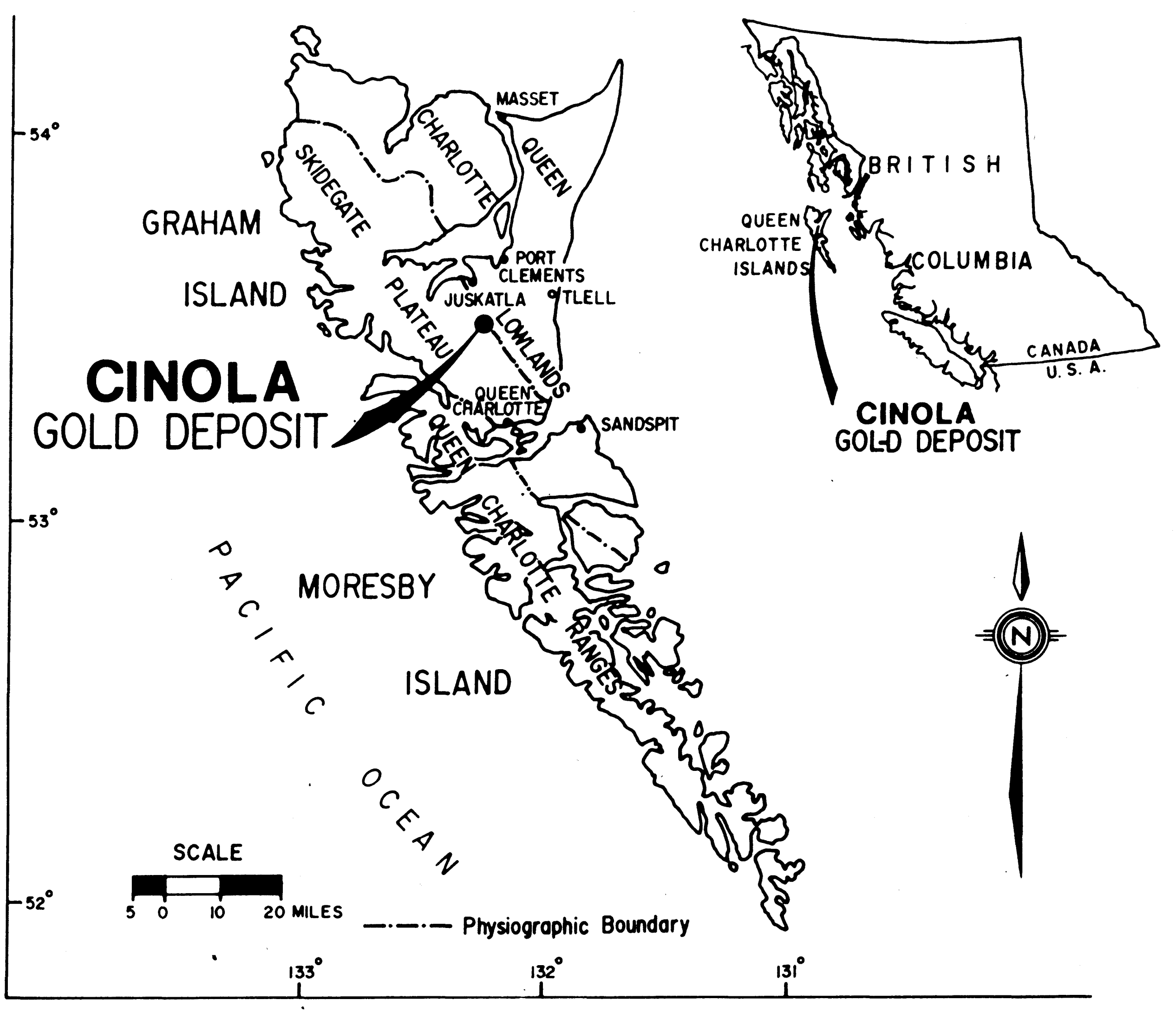

FIGURE 1. Location of the Cinola gold deposit, Queen Charlotte Islands, B.C.

TABLE 1. Table of geologic formations, Queen Charlotte Islands

PLEISTOCENE-RECENT		glacial and interglacial sediments
LATE TERTIARY		SKONUN FM: marine and non-marine sands
EARLY TO MIDDLE TERTIARY		MASSET FM: alkali basalt floods and sodic rhyolite ash flows
LATE CRETACEOUS	QUEEN CHARLOTTE GROUP	SKIDEGATE FM: marine sandstones and siltstones
		HONNA FM: conglomerates
		HAIDA FM: marine sandstones and shales
EARLY CRETACEOUS		LONGARM FM: marine lithic wackes and calcareous siltstones
UPPER TRIASSIC TO LATE JURASSIC	VANCOUVER GROUP	YAKOUN FM (M. JURASSIC): explosive andesitic volcanics
		MAUDE FM (L. JURASSIC): marine shales and sandstones
		KUNGA FM (L. JURASSIC AND UPPER TRIASSIC): limestones
		KARMUTSEN FM (U. TRIASSIC) mafic volcanics

Au/tonne. This includes 10% dilution from the walls of the orebody and from included waste. Silver grade is about the same as gold. Sutherland Brown and Schroeter (1975) were the first to describe the showings formally and produced a generalized geological cross section of the deposit. Richards *et al.* (1976, 1979) classified the deposit as Carlin-type and published the first K-Ar age determination. Champigny and Sinclair (1980) published a more detailed description of the geology based on preliminary interpretation of surface and drill-hole data obtained to the end of August 1979.

This account is based on geological examination of 5506 m of diamond drill core and limited surface exposure during the summer of 1979 followed by laboratory studies at the University of British Colulmbia. Computer-oriented core logging techniques (GEOLOG system) were used as a basis for the field work (Blanchet and Godwin, 1972; Godwin *et al.*, 1977).

Regional Geology

The Queen Charlotte Islands are part of the Insular Tectonic Belt of the Canadian Cordillera and are composed of rocks ranging in age from Late Triassic to Recent (Sutherland Brown, 1968) (Table 1). Three major periods of volcanism are recognized that separate four principal episodes of sedimentation. Plutonism seems to be confined to two main periods. Bodies of hornblende diorite to quartz diorite composition were emplaced in the Middle to Late Jurassic and a more varied sequence of quartz diorite to alkaline granitic rocks was intruded in the Early to Middle Tertiary. Crustal fracturing, mainly along major northwest-trending faults, has had a pronounced effect on volcanism, sedimentation, intrusion and secondary folding (Sutherland Brown, 1968).

The general area of the Cinola gold deposit is underlain by three main rock units, the Haida Formation of Late Cretaceous age, the Masset Formation of Early to Middle Tertiary age and the Skonun Formation of middle Miocene age (Fig. 2). These rocks are cut by the Sandspit fault system of regional extent (Sutherland Brown, 1968). The Sandspit fault system separates the two main physiographic provinces of the area, the Queen Charlotte Lowlands on the east and the Skidegate Plateau to the west. The fault zone strikes about 143 degrees and seems to have a large vertical movement. Southwest of the deposit, the Haida Formation is mainly shales. The Skonun Formation overlies the Haida Formation unconformably and is a conglomerate with coarse pebbles to small cobbles, coarse sandstone and minor siltstone or shale. West of the Cinola deposit, volcanic rocks of the Masset Formation mark the beginning of the Skidegate Plateau. Near the Cinola deposit, Masset volcanic rocks are mainly olivine basalt.

Stratigraphy

The deposit underlies a small hill (210 m above sea level) in the transition zone between the Skidegate Plateau and the Queen Charlotte Lowlands. Shale of the Haida Formation and an overlying interbedded sequence of pebble conglomerate and coarse sandstone of the Skonun Formation are both intruded by an elongate stock of porphyritic rhyolite (Fig. 3). A thin cover of glacial till and sand overlies the area and outcrops are scarce in the vicinity of the deposit.

Shale (Haida Formation, Late Cretaceous)

The Haida formation underlies an area from the Tertiary volcanic rocks on the west side of the deposit to the overlying coarse clastic rocks to the east. Thickness of the shale at the Cinola deposit is unknown, although a maximum thickness of 34 m was penetrated in one drill hole. The rock is mainly a dark grey to black, poorly consolidated and thinly bedded calcareous shale. Minor sandy layers are present. Near the contact with the porphyritic rhyolite, the shale becomes an argillite or hornfels because of intense silicification. On the basis of lithology, this shale appears to correlate with the upper member of the Haida Formation.

Conglomerate and Sandstone of the Skonun Formation (Miocene)

Coarse-grained sedimentary rocks overlie the Haida shale and extend eastward to the Sandspit fault (Fig. 3). The contact between the two units has not been observed clearly in drill core because of pervasive silicification and intrusion of the porphyritic rhyolite (Figs. 3, 4 and 5). Thickness of the sequence throughout the area drilled varies from 0 to 300 m. The strike changes from northwest to northeast, with most of the strikes near 015°. Strata consistently dip 15 to 25 degrees to the east. The thickness of individual conglomerate, sandstone or siltstone layers is from 0.1 to 30 m, with a 2-m average. The sequence contains about 62% conglomerate, 26% coarse sandstone, 7% intercalated sandstone and siltstone with rare shale interbeds, and 5% matrix-supported conglomerate. Basal contacts of the beds are generally sharp, but rare transitional contacts are also observed. Mafic volcanic, pebble-rich conglomerate, interbedded sandstone and shaley siltstone and some sandstone have been used successfully for stratigraphic correlation among drill holes, as is apparent in Figures 4 and 5.

The principal rock type is a medium grey to pale brown polymictic conglomerate with well-rounded to subangular large pebbles and small cobbles. Graded bedding and load cast structures are abundant. The coarse fraction totals 70% of the rock, with an average fragment diameter of 3 cm. Particles are moderately sorted and sphericity is low to intermediate. Most of the conglomerate units are pebble supported. Pebbles and cobbles are 60% felsic volcanic rock, 20% mafic volcanic rock, 10% granite, 5% argillite and shale, and 5% conglomerate, sandstone, siltstone and chlorite schist. Felsic volcanic clasts include massive and banded rhyolite, porphyritic rhyolite, quartz and rare pyroclastics, chert and hematitic porphyritic rhyolite. Mafic volcanic pebbles are mostly dark green porphyritic andesite, with plagioclase and hornblende phenocrysts commonly altered to chlorite and epidote. Granitic fragments consist of a quartz-feldspar mosaic with about 10% disseminated biotite or chlorite. Rare wood fragments are intermixed with the coarse and fine fractions. The matrix of these conglomerates occupies 30% of the volume of the rock and consists of sand-sized particles of quartz and rock fragments. Distinguishing quartz cement from quartz clasts is difficult in most of the samples because of the poor definition of quartz clast boundaries. The mosaic and sutured contacts suggest that recrystallization during mineralization may have destroyed many original clast boundaries.

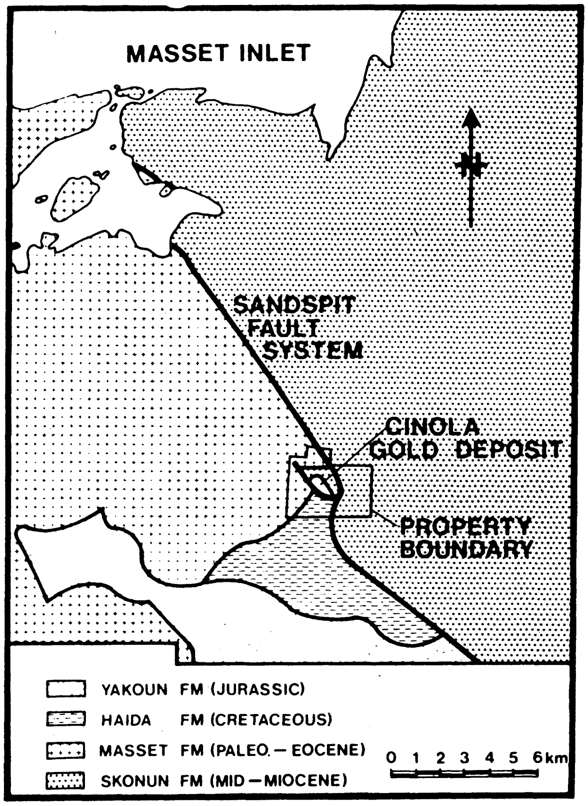

FIGURE 2. Regional geology, Cinola gold deposit (after Sutherland Brown, 1968).

Sandstones are medium grey to dark brown and medium to coarse grained, with bedding and graded bedding common. Quartz and volcanic rock fragments comprise most of the grains. Two to 15% wood fragments are present, commonly aligned parallel to bedding. Leaves have been found in sandstone units. One small outcrop of sandstone contains abundant well-preserved pelecypods. The shells are relatively thick and most of them are flat lying. One spheroidal concretion was observed in a sandstone bed.

Minor but persistent medium to pale grey interbedded sandstone and siltstone-shale occur throughout the deposit. They have bedding, graded bedding, cross-bedding, ripple marks, and rare convolute bedding and flame structures.

Massive, matrix-supported conglomerate occurs locally. These consist of angular fragments of sandstone and conglomerate in a matrix of silty mud.

Similar rock types and types of clasts, the abundance of carbonaceous material and the regional stratigraphic setting sug-

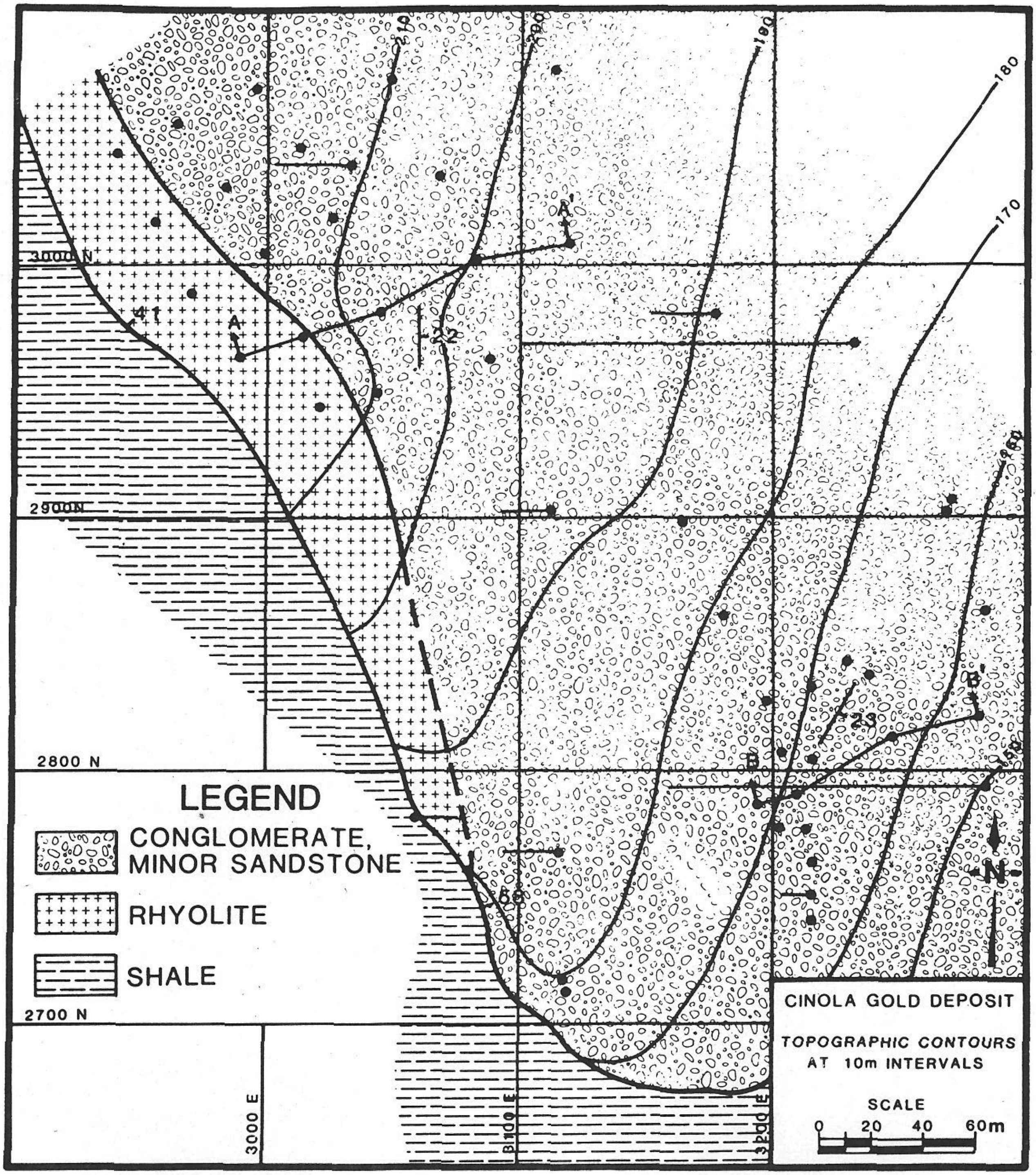

FIGURE 3. Property geology, Cinola gold deposit. Topographic contours in metres a.m.s.l. are shown only on the east side of the Footwall fault, which separates shale from the other two units. AA′ and BB′ are locations of cross sections in Figures 4 and 5.

gest that this sedimentary sequence correlates with the basal part of the Skonun Formation of Middle Miocene age in the lower part of the Tow Hill well (Sutherland Brown, 1968, p. 120) to the northeast. The designation of this coarse clastic sequence pyroclastic material by previous geologists is misleading in the light of our detailed megascopic and microscopic studies. An epiclastic volcanic component does occur with other fragment types. No relict textures were seen which would indicate the presence of a pre-existing pumice or rhyolite as reported by Cruson and Limbach (personal communication, 1980).

Environment of Deposition and Age of Skonun Sediments

The coarse nature of the sediments, their polymictic character and erosional contacts between conglomerate and sandstone units strongly suggest a fluviatile environment of deposition for the Skonun sediments, either as meandering or braided river deposits (Blatt *et al.*, 1972, p. 199). In sediments deposited by meandering rivers, framework conglomerates are uncommon and occur only as localized lag concentrates. In contrast, framework conglomerates dominate the sediments

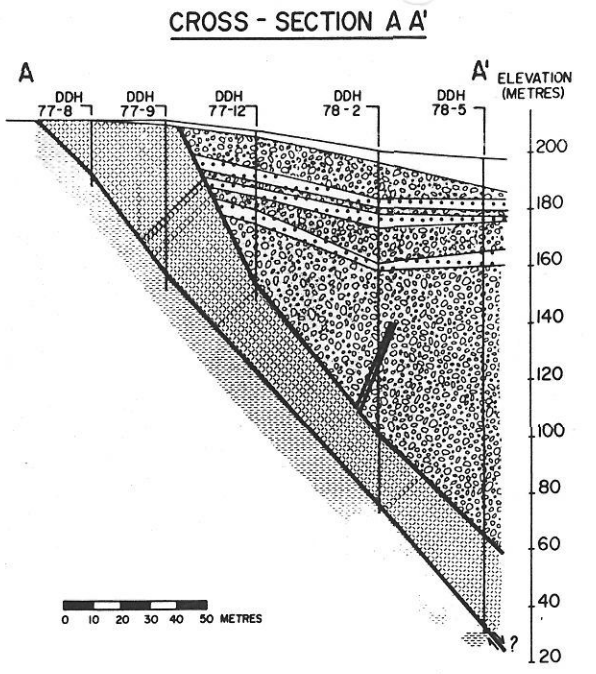

FIGURE 4. Cross section AA'. Location shown on Figure 3. See Figure 5 for legend.

TABLE 2. Lithofacies and sedimentary structures observed in the Skonun sedimentary rocks of the Cinola gold deposit and other braided river systems.

Approx. % Tot. Sed. Vol	Lithofacies	Sedimentary Structures Observed	Interpre-tation
62	massive or crudely bedded framework conglomerate	-graded bedding -rare horizontal bedding	channel deposits
26	sandstone, medium to very coarse, may be pebbly	-horizontal lamination -wood fragments	channel deposits
7	sand, silt, mud	-fine lamination cross lamination ripple marks -pelecypods	overbank or waning flood deposits
5	massive matrix-supported conglomerate	none	debris flow deposits

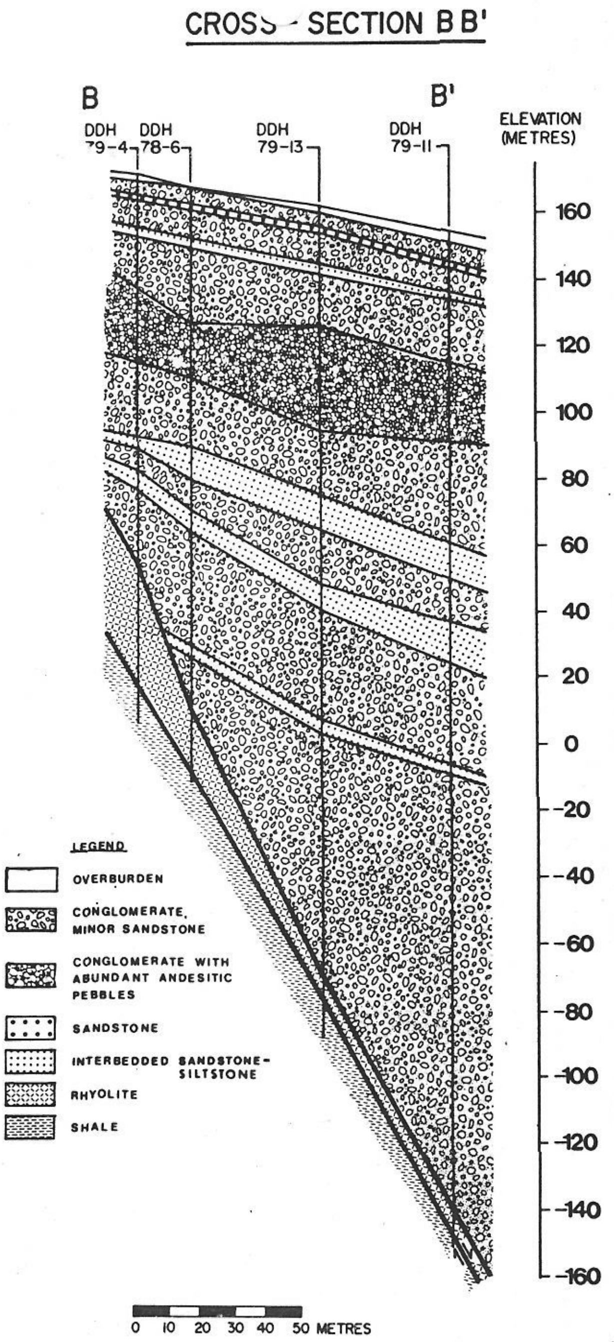

FIGURE 5. Cross section BB'. Location shown on Figure 3.

deposited in modern braided rivers. Framework conglomerate is the dominant lithofacies at the Cinola deposit and, according to Rust (1978), is evidence for deposition by a braided river system. Rust (1978), Miall (1978), and Vondra and Burggraff (1978) describe distal braided river and alluvial plain sequences very similar to the sedimentary rocks of the Skonun Formation present at the Cinola deposit. Table 2 is a list of the lithofacies and sedimentary structures observed both at the Cinola deposit and in recognized distal braided river and alluvial plain deposits.

Conglomerate and sandstone make up 85 to 90% of the total sedimentary rock volume, the remainder consisting of silty mudstone and minor shale. Conglomerate and sandstone are interpreted as deposits of the active tract, whereas mudstone and plant fragments accumulated on inactive areas. The active tract migrated across the floodplain; the area eventually became inactive and accumulation of mud and support vegetation began, although minor channels still remained to transport sand during flood periods.

Much of the detritus found in the fluviatile sequence is most likely to have been derived and transported eastward from the Early to Middle Tertiary volcanic rocks of the Masset Formation. The coarse clasts are mostly rhyolite, quartz-feldspar porphyry and porphyritic andesite, all of which, except porphyritic andesite, are very common in exposures of the Masset Formation. Jurassic andesitic agglomerates, Upper Cretaceous shales and intrusions could be the sources for chloritized andesitic, argillite and granitic clasts respectively.

Rust (1972) found framework gravel 50 km from the river's source in a comparable fluviatile sequence. The occurrence of boulder-sized rock fragments, the presence of some debris flow and the proximity of the probable source area suggest a distance of transport much shorter than 50 km, although most of the Skonun rocks appear distal.

A sample of carbonaceous siltstone with abundant pyrite was collected by the authors in the eastern part of the deposit (drill hole 79-14) and submitted for palynological analysis. In addition, three samples of shelly sandstone were collected in a

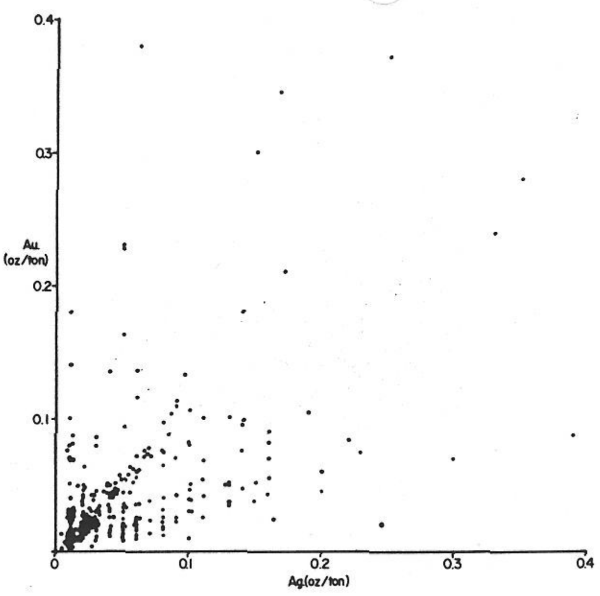

FIGURE 6. Gold-silver scatter diagram for "low-grade" assays from drill core, based largely on 2-m core lengths.

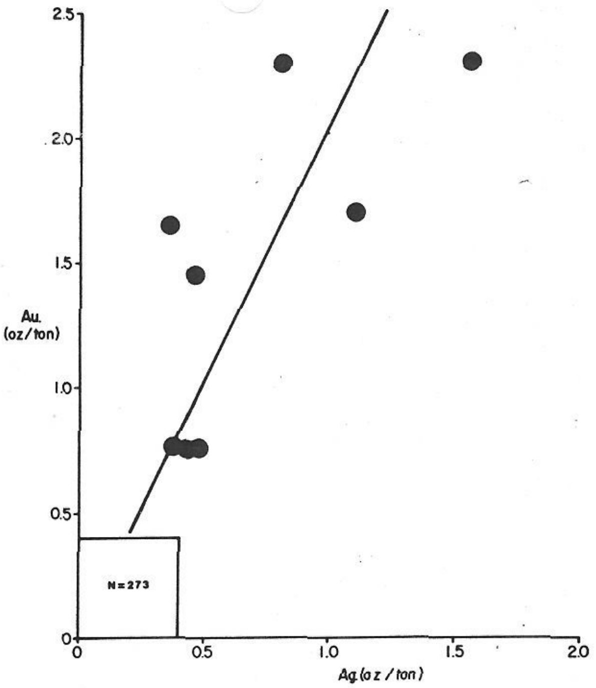

FIGURE 7. Gold-silver scatter diagram for "high-grade" assays (higher than 0.4 oz Au/ton), based on 2-m core lengths.

surface trench. The plant microfossil assemblage and fauna reveal an early Middle Miocene age (17-15 Ma) for the deposition of the Skonun (Champigny *et al.*, 1981). The suggested environment of deposition is that of a near-shore, possibly estuarine environment, which is in accord with the sedimentological interpretation proposed here.

Porphyritic Rhyolite (Middle Miocene)

An elongate stock of porphyritic rhyolite and associated dykes crops out sparsely east and west of the Footwall fault. The intrusion cuts both the shale and the conglomerate and sandstone. Locally, the contact with the coarse sedimentary rocks is sharp, but in many places a transition zone exists. The contact zone is composed of a mixture of very deformed conglomerate, sandstone and rhyolite fragments in an aphanitic white to bluish grey siliceous matrix. The thickness of the porphyritic rhyolite mass decreases to the east (Figs. 4 and 5). The rock is pale grey and contains 1 to 3% bluish-grey subrounded quartz eyes, 0.1 to 4 mm in diameter, and 5 to 8% white subhedral to euhedral feldspar phenocrysts, 0.1 to 5 mm long.

Plagioclase phenocrysts, mainly albite, are more abundant than potassium feldspar phenocrysts. The rhyolite is brecciated in many places, with angular fragments of rhyolite and shale contained in a very fine-grained matrix of dark grey to black silicified shale. In the conglomerate close to the intrusive mass, angular fragments representing broken pebbles are visible. These breccias are probably related to the intrusion of the porphyritic rhyolite.

Recent K-Ar data on the Tertiary volcanic rocks of the Masset Formation compiled by Young and Chase (1976) resulted in a revision of their age. Sutherland Brown's (1968) interpretation and his single K-Ar analysis gave a Paleocene to Eocene age. Nineteen recent whole-rock K-Ar analyses provide ages ranging from 11 to 84 Ma. At least two interpretations are possible from these data: (1) there is more than one Tertiary volcanic cycle or (2) the younger ages are reset from Early Tertiary ages. If we accept the first interpretation, then the porphyritic rhyolite intrusion could represent a plutonic phase associated with a Late Tertiary volcanic cycle. The Sandspit fault system probably also played an important role in the localization and form of the porphyritic rhyolite stock.

Structure

The major structural feature on the Cinola gold deposit is the Footwall fault, which strikes 180 to 157 degrees and dips 53 degrees to the east (Figs. 4 and 5). The Footwall fault parallels the Sandspit fault system and probably is a part of that system. In the drill core, the Footwall fault is recognized by: (1) an abrupt change from silicified shale to soft, fresh shale and (2) slickensides in altered porphyritic rhyolite and silicified shale. In the northwest part of the deposit, an outcrop called the Marino showing exposes the fault contact. Also, on surface, the fault is visible as a fault scarp near the southwest boundary of the deposit (Fig. 3).

The porphyritic rhyolite is exposed both beneath and above the Footwall fault. Thus, faulting occurred at least in part after intrusion of the porphyritic rhyolite. The absence of Middle Miocene sedimentary rocks on the west side of the Footwall fault and displaced geochemical anomalies and drainage patterns suggest a dextral fault with some relative downward movement of the east block. This is the same sense of movement as observed for the Sandspit fault system (Sutherland Brown, 1968, p. 153).

Tow Hill well, drilled on the eastern block of the Sandspit fault in the late 1950s intersected the base of a conglomerate-sandstone sequence at 1800 m b.m.s.l. (Sutherland Brown, 1968). The Skonun sedimentary rocks are exposed on the west side of the Sandspit fault system at the Cinola deposit at a minimum elevation near -200 m. Gravity measurements by Young and Chase (1976) give a dip for the Sandspit fault of 50 to 70 degrees east and a vertical displacement of approximately 1500 m (east block down). This compares well with a vertical difference of 1600 m between the Skonun sedimentary rocks of the Cinola deposit and the Tow Hill well. The Footwall fault on the Cinola gold deposit has been active after the intrusion of the porphyritic rhyolite; that is, after 14 Ma. The similar strike, dip and movement of the Footwall fault and the Sandspit fault strongly suggest that the two result from the same stress pattern.

Form and Setting of the Cinola Deposit

The Cinola deposit, extending over an area of at least 1.3 km^2, appears to terminate abruptly against the Footwall fault on the west and disappears gradually to the north and east (Fig. 3). The depth extent is unknown, but is at least 350 m. In size and shape, the mineralized system rivals small porphyry systems and is characterized by a prominent zone ilicification with a few per cent of pyrite and marcasite. Gold and silver are widespread over the same area. Gold is between 0.03 and 156 g Au/tonne. High-grade gold (i.e., more than 7 g Au/tonne) occurs in quartz veins sporadically throughout the deposit and in quartz veinlets at the contact zone between the porphyritic rhyolite and the Skonun conglomerates (Fig. 8). The rocks are highly anomalous in mercury and arsenic and less anomalous in antimony and tungsten.

Intense silicification characterizes the host rocks. The degree of silicification increases in a general way toward the porphyritic rhyolite body. Several generations of veins and stringers cross-cut the host rock.

Large veins up to several metres wide strike 020 to 202 degrees and dip 60 to 90 degrees in either direction. Increasing spatial density of quartz veins near mineralized rhyolites has been measured quantitatively in most drill holes (Fig. 8). Individual veins present clear accretionary features, such as crustification, chalcedonic quartz and development of well-formed quartz and calcite crystals up to 2 cm in size, with coxcomb textures in drusy cavities. Banding in the veins is common; several coloured bands of quartz show the different episodes of veining. Microveins and stringers commonly pervade wood fragments, producing a chessboard texture on a hand-specimen scale. Cross-cutting relationships support the following sequence of veining in order of decreasing age: a) black to grey chalcedonic quartz, b) hematitic quartz, c) massive milky quartz, d) clear euhedral quartz and e) calcite.

Wall-rock silicification is common and in many places conglomerate clasts are brecciated and incorporated within a quartz vein. This is seen only with black and grey quartz veins. It is generally difficult to distinguish between vein material and host rock.

Wall-Rock Alteration

Alteration minerals identified in drill core and thin sections include, in decreasing order of abundance; quartz, illite, *kaolinite, sericite and chlorite.* Iron hydroxides are also present near the surface.

Quartz is the predominant mineral and is present in two generations; (1) a first generation of cryptocrystalline quartz cement binding pebbles and smaller clasts of the original sediment and (2) a second generation of blocky clear crystals, 0.1 mm to 2 cm in diameter, as void fillings, vugs and veins. This later generation corresponds to the sequence of mineralization described elsewhere in this account. This second generation of quartz is clearly related to gold mineralization. Thus, two periods of silicification have affected the original sediment.

Quartz cement has corroded parts of lithic clasts and produced quartz overgrowth. Cementation destroyed the clast boundaries, which locally are reduced to an iron oxide rim. Quartz cement commonly rims pyrite grains and carbonaceous fragments.

In quartz veins, coxcomb structure is common. In numerous veins, thin selvages of quartz are coated with pyrite, which in turn is covered with drusy quartz crystals projecting to the interior of the vein where they are encased in pyrite crystals. This common texture shows that quartz deposition in part preceded formation of all opaque minerals and continued to some extent during deposition of opaque minerals. Plagioclase phenocrysts of the porphyritic rhyolite are replaced in many places by quartz.

Argillic alteration is extensive. Illite and kaolinite are the two clay minerals identified by X-ray diffraction. These clays seem to be the result of hydrothermal alteration, based on their random orientation and fibrous habit in the mineralized rocks. Illite and kaolinite occur: (1) with quartz cement in the matrix of rhyolites, conglomerates, sandstones and siltstones, (2) as void and vein fillings, commonly coating quartz crystals, and (3) as alteration products of feldspar phenocrysts.

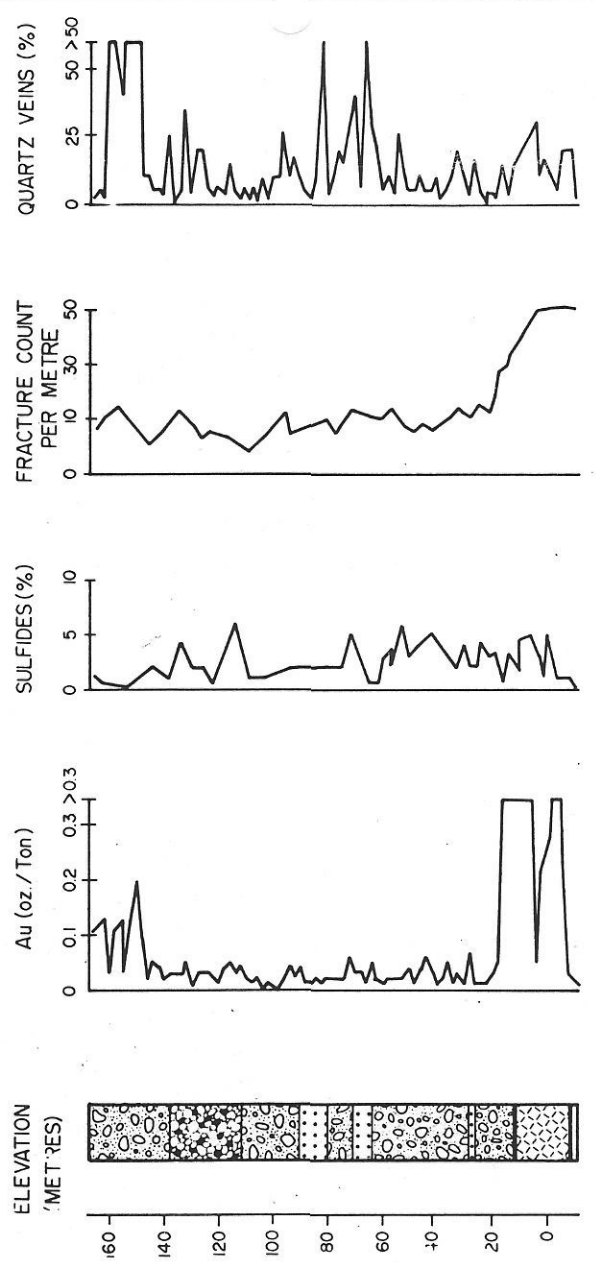

FIGURE 8. Graphic log of diamond drill hole 78-6. See Figure 5 for location and legend.

Clusters of idiomorphic pyrite crystals are found in clay-altered rocks. At the contact zone between the Miocene sedimentary rocks and the porphyritic rhyolite, argillically altered sedimentary rocks are silicified with very fine-grained quartz. This superimposed silicification on argillic alteration has been referred to as an advanced argillic alteration in porphyry-copper deposits by McMillan and Panteleyev (1980). These observations suggest that illitization and kaolinization took place during and after quartz and sulphide deposition. Taylor and Fryer (1980) observed that phyllic overprinting affected all primary minerals except quartz and pyrite, which is also the case with the argillic alteration at Cinola.

A zone of argillic alteration, in which more than 30% of the gold-bearing rock is composed of clay, constitutes the eastern boundary of the mineralization (Fig. 10). This argillized zone dips steeply to the west and, in general, gold is less than 0.4 g/tonne.

Sericitic alteration occurs mainly as finely disseminated grains on the feldspar phenocrysts of conglomerate pebbles and of the porphyritic rhyolite. Small amounts also occur in the matrix of rhyolites, conglomerates and fine-grained

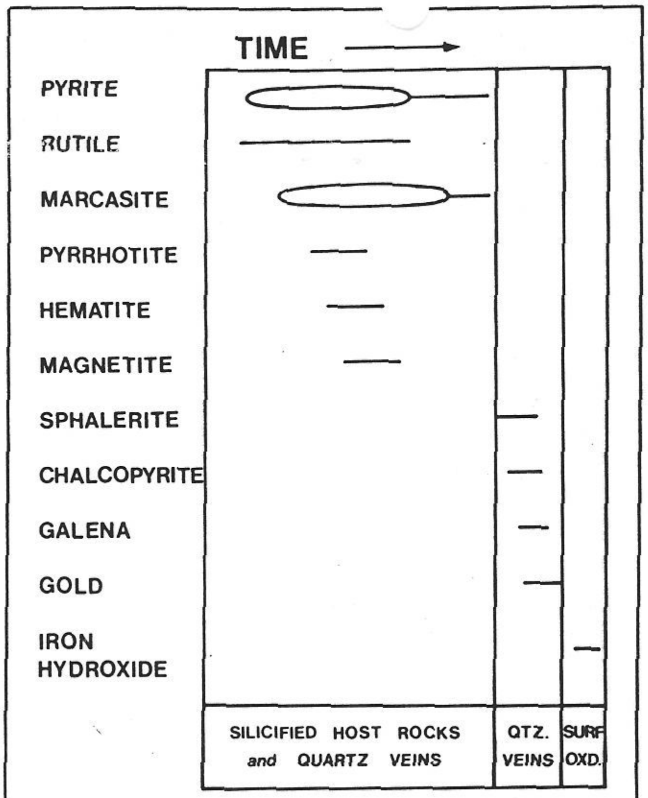

FIGURE 9. Paragenetic line diagram for the Cinola gold deposit's opaque minerals.

sedimentary rocks, and silicified shales. An earlier phyllic zone could have been present around the intrusion, but the pervasive nature of the argillic alteration makes recognition of any early alteration stage very difficult if not impossible.

Except for alteration of phenocrysts in andesitic pebbles in conglomerate, chlorite seem to be limited to the contact zone of the porphyritic rhyolite, where the mineral is finely disseminated with quartz, illite and kaolinite. Chlorite might represent: (1) an alteration product of a glassy chilled margin of the rhyolite intrusion or (2) a mineral phase related to early hydrothermal alteration.

Iron hydroxides are present on surface exposures and up to 20 m in depth in drill holes. They form pale yellow to reddish brown fine-grained earthy material filling and lining boxwork cavities and veinlets. They result from oxidation of pre-existing sulphide minerals, principally pyrite and marcasite.

Ore. Mineralogy

Opaque minerals recognized in the Cinola deposit are listed in Table 4, with an indication of their approximate abundances in 60 specimens examined in detail. Mineralized rock contained from 0.5 to 10% opaque minerals, with an average of about 3% (by volume). Two general mineral associations are present in the deposit (Figs. 9 and 12): pyrite-marcasite in silicified host rocks and pyrite-marcasite-sphalerite-chalcopyrite-galena and native gold in quartz veins.

Pyrite and marcasite are the most common metallic minerals. Four generations of pyrite are present. In order of decreasing age they are: (1) "raspberry-like" pyrite, rarely observed and possibly of sedimentary origin, (2) fine-grained melnikovitic pyrite occurring as coatings and fissure fillings in pebbles of conglomerates, (3) well-developed single crystals or crystal clusters in the coarse fraction and cement of the

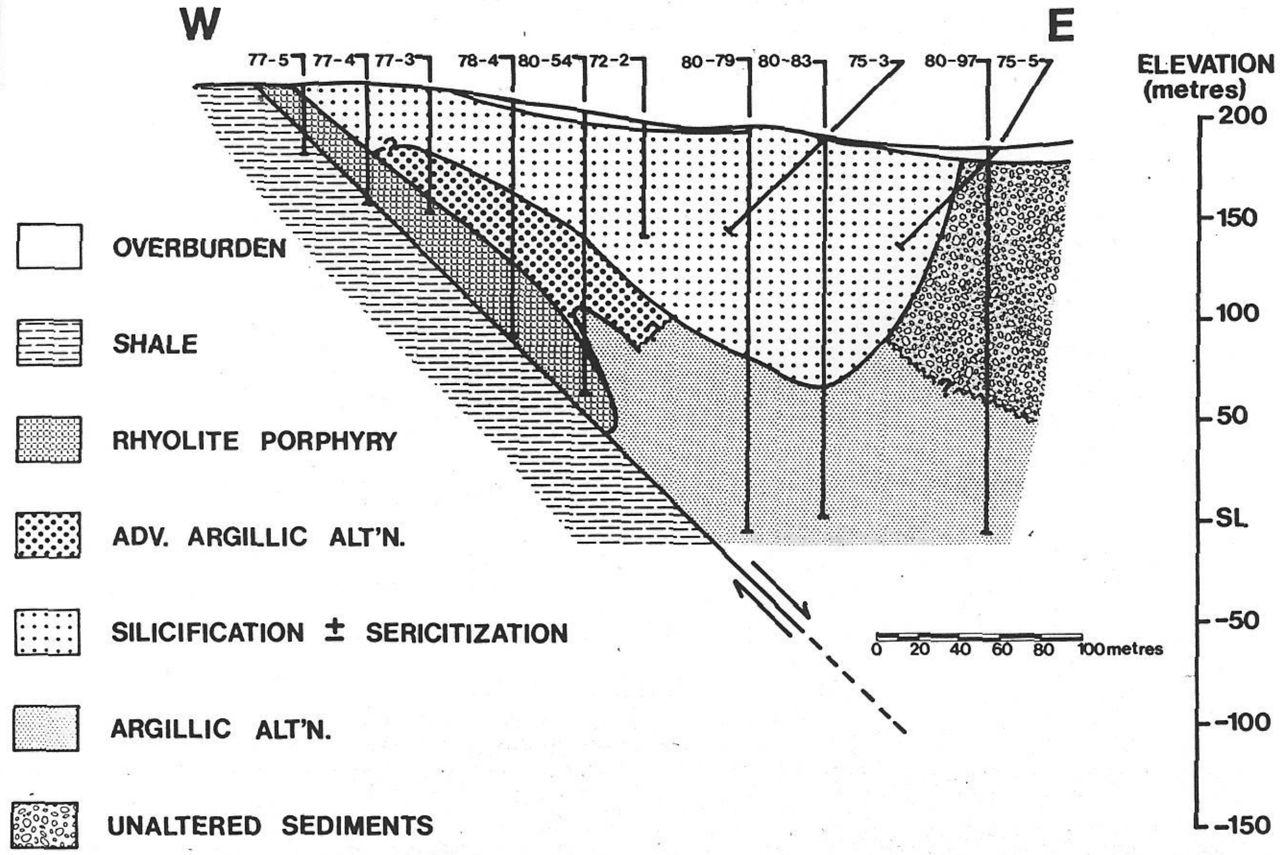

FIGURE 10. Cross section showing distribution of alteration minerals of the Cinola gold deposit. Argillic alteration indicates that the sediment is composed of more than 30% clays (illite and kaolinite). Grades in the argillic alteration zone are less than .4 g/tonne. Advanced argillic alteration signifies that silicification is superimposed on argillic alteration. The rhyolite porphyry and the shale within a few metres of the fault contact are silicified, sericitized and gold-bearing.

silicified sedimentary rocks, and (4) pyr[illegible]n quartz veins and vugs, where it is disseminated or forms layers in cryptocrystalline quartz. Pyrite and marcasite occur individually or together. Individual grains range from .01 to 4 mm. Sulphide rims around pebbles in the conglomeratic host consist of disseminated pyrite grains (.001 to .05 mm). Marcasite commonly forms groups of small lath-shaped crystals and in places has the characteristic coxcomb form. Quartz, pyrite and marcasite have filled spaces in wood fragments. Graphite was observed rarely with the organic matter. In conglomerate, pyrite and marcasite are distributed through both the matrix and pebbles, indicating a deposition subsequent to the formation of the sediment. No definite correlation can be obtained between sulphide minerals and gold abundances (Fig. 8).

Inclusions of pyrrhotite, hematite and rarely magnetite and rutile were observed in pyrite grains. Five pyrite-marcasite grains were analyzed with the electron microprobe and in one grain there is 1.1 weight per cent arsenic. No arsenopyrite has been identified in the deposit and the high arsenic content can probably be attributed to solid solution of arsenic in either or both of pyrite and marcasite.

Rutile occurs as lath-shaped disseminated grains or aggregates. Grains are relatively small; around .02 mm. No other metallic minerals are in contact with rutile, apart from abundant pyrite. Rutile could have been a primary mineral, as it is not found in quartz veins.

Small amounts of pyrrhotite are inclusions from .01 to .03 mm in diameter in pyrite and marcasite. Hematite occurs as finely disseminated grains (<.005 mm) in quartz veins, giving a brownish red colour to the quartz. Trace amounts of hematite are inclusions (.01 to 0.1 mm) in pyrite or marcasite. Magnetite is very rare and as anhedral to euhedral grains from .02 to .3 mm in size included in pyrite and on one sample as an inclusion in cinnabar. Mercury minerals (cinnabar and tiemannite, HgSe) were observed in one quartz vein sample. Cinnabar is present as .01- to .05-mm disseminated patches in quartz. "Framboidal-like" pyrite is associated with cinnabar in several places.

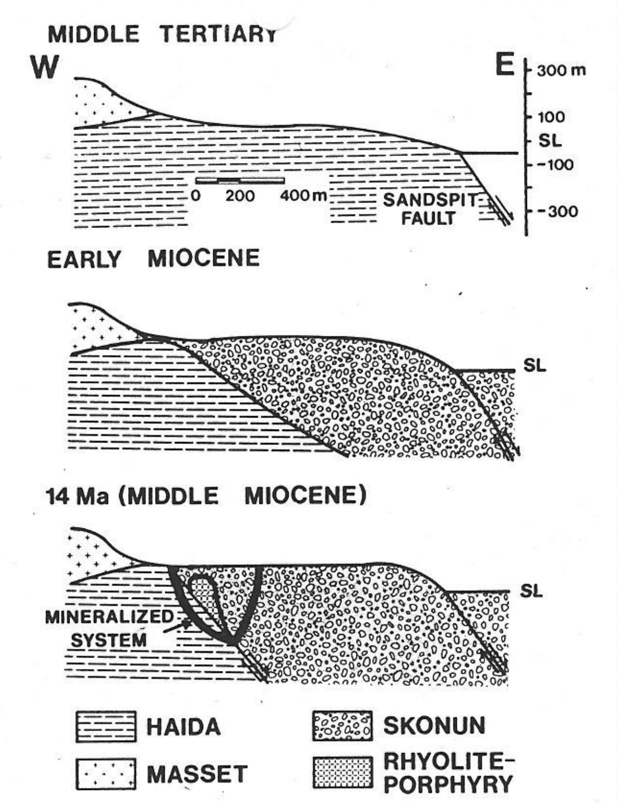

FIGURE 11. Schematic sequence in the development of the Cinola gold deposit. Erosion of the Haida shales during early Miocene is speculative. Emplacement of rhyolite porphyry is thought to have initiated thermal convection of pore water from the Skonun Formation and led to development of the mineralized system. See text for details.

Sphalerite is present only rarely, but is the most abundant sulphide mineral after pyrite and marcasite. It is encountered only in quartz veins generally in contact with pyrite, marcasite, chalcopyrite, galena and gold. Grains are generally irregular and their size varies from .01 to .02 mm. Sphalerite has been observed with inclusions of pyrite, chalcopyrite, galena and quartz, but many grains are clear of inclusions. Molecular per cent FeS in sphalerite obtained from seven electron microprobe analyses ranges from 11 to 25, indicating that sphalerite in the Cinola deposit is iron-rich. Chalcopyrite is less abundant than sphalerite and is closely associated with sphalerite either as inclusions or as simple composite or monomineralic sulphide grains. Grain size is comparable to sphalerite. All chalcopyrite grains are irregular. Thin veinlets of chalcopyrite cross-cut sphalerite grains. Rounded inclusions of native gold in chalcopyrite were observed in a few places. Galena is very rare and is in polymineralic aggregates with sphalerite, chalcopyrite and gold; grains are .01 to 0.1 mm in size. One veinlet of galena was seen cross-cutting a sphalerite grain. From 20 to 23 molecular per cent Se was recorded in three electron microprobe analyses of galena grains, so the mineral is actually in the galena-clausthalite solid solution series. Native gold occurs in three principal ways: (1) micron-gold in all the rock types that have undergone silicification (quartz veins included), (2) as monomineralic grains in quartz veins and (3) included in chalcopyrite in quartz veins. The third association is found only locally. The visible gold grains (>10 μm) are very irregular, with some as large as 500 μm. Inclusions of gold

TABLE 3. Analytical data and K/Ar model ages, Cinola gold deposit

Sample Identification	Rock Type	%K $\pm \sigma^b$	^{40}Ar (rad) / ^{40}Ar (total)	^{40}Ar (rad) (10^{-7}cm^3 STP/g)	Apparent Age (ma)^c
22065 M^a	Silicified Rhyolite Porphyry	1.19±0.04	.532	6.522	14.0±0.6
7906 DO1	Silicified Rhyolite Porphyry	5.31±0.12	.440	29.22	14.1±0.6
7805 DO1	Silicified Shale (Haida Formation)	2.19±0.04	.505	14.85	17.4±0.5

a, Results provided courtesy of N.C. Carter and G.G. Richards
b, error is one standard deviation (laboratory measurement error)
c, constants used for model age calculations: $\lambda_\alpha = 0.581 \times 10^{-10}$ year^{-1}
$\lambda_\beta = 4.96 \times 10^{-10}$ year^{-1}
$^{40}K/K = 1.167 \times 10^{-4}$

TABLE 4. Opaque minerals and their relative abundance (out of 100 vol. % opaque minerals), Cinola gold deposit; trace amounts means less than 0.1 volume per cent

Mineral	Silicified Host Rock	Quartz Veins
Pyrite	75	75
Marcasite	22	22
Rutile	2	—
Pyrrhotite	0.5	0.5
Hematite	0.5	2.5
Magnetite	tr	tr
Sphalerite	—	tr
Chalcopyrite	—	tr
Galena	—	tr
Gold	not visible	tr
Cinnabar	—	tr
Tiemannite	—	tr

in chalcopyrite are 10 μm on average and are more-or-less rounded.

Eleven visible gold grains (>100 μm) occurring in quartz veins were analyzed with the electron microprobe. All the gold contains silver, ranging from 6.2 to 76.4 weight per cent. The calculated Au/Ag varies from 0.2 to 15.1, with an average and standard deviation of 6.3 and 4.9 respectively. These results contrast somewhat with gold-silver scatter diagrams for assays from drill core (Figs. 6 and 7), which on average have about twice as much gold as silver. Nevertheless, we conclude that: (1) virtually all the silver is in solid solution with gold and (2) silver minerals other than gold-silver solid solution are unlikely to occur. None have been found to date. The trace amounts of galena present may contain some silver. One gold analysis has 9.8 weight per cent Te in a grain abnormally enriched in silver (wt. % Ag = 76.4).

Age of Mineralization

The intrusion of porphyritic rhyolite and gold mineralization are closely related in space, time and perhaps genesis. Quartz veins of the mineralizing system cut the porphyritic rhyolite near its eastern margin, indicating that at least some mineralization took place after the emplacement of the rhyolite intrusion.

Ages of two samples of gold-bearing silicified porphyritic rhyolite and one sample of gold-bearing silicified shale were determined by the K/Ar method (Table 3). All three samples contained about 1% disseminated pyrite. A 17.4-Ma model age was obtained for silicified shale adjacent to the porphyritic rhyolite and represents a reset or partially reset age of the Late Cretaceous shale. Thus, the model age appears to be a maximum possible age of emplacement of the porphyritic rhyolite, a conclusion in accord with the early Middle Miocene age indicated by palynology for the Skonun Formation, which is cut by the porphyritic rhyolite (Champigny *et al.*, 1981). The two 14-Ma model ages for silicified and sericitized porphyritic rhyolite almost certainly represent the age of mineralization as well as the minimum age of emplacement of the porphyritic rhyolite. These data indicate that both intrusive and mineralizing events were confined to a maximum interval of about 3 million years. We favour an interpretation in which 14 Ma represents the time of both intrusion and mineralization, and the 17.4-Ma model age was not completely reset by heat from the porphyritic rhyolite or the mineralizing fluids.

Classification of the Cinola Deposit

Richards *et al.* (1976) consider the deposit to be of the Carlin type, a conclusion supported by the authors' observations. Features in common with the gold deposits of north-central Nevada (Carlin, Cortez, Getchell and Gold Acres) are: (1) small particle size for most of the gold, (2) Tertiary age of mineralization (14 Ma in the case of the Cinola deposit), (3) trace-element abundances, in particular high Hg, As and Sb, (4) argillic alteration, (5) association with major high-angle faults, (6) high porosity and permeability of the host rock (mostly uncemented conglomerate and sandstone at Cinola), (7) close spatial association with felsic intrusions and (8) low silver content.

Genetic Model

A general model for the evolution of host rocks and genesis of the Cinola gold deposit includes three main events (Fig. 11): (1) in the Middle Tertiary, extrusion of Masset volcanic rocks over Haida shales and activation of, or continuation of, movement along the Sandspit fault; (2) in the early Middle Miocene, uplift and erosion of Masset volcanic and older rocks and subsequent deposition of Skonun conglomerates, sandstones and siltstones; and (3) at 14 Ma, intrusion of the porphyritic rhyolite stock along the Footwall fault, followed by the development of a fracture system that provided structural control of mineralization and physical limits to the mineralizing system.

The pre-mineralization Skonun Formation is viewed as a permeable, water-saturated pile of clastic sediments. Initiation of faulting along the Footwall fault, a part of the Sandspit fault system, controlled emplacement of an elongate stock of rhyolite-porphyry at about 14 Ma. This event upset the preexisting thermal regime, and initiated the development of convection cells in pore water in the Skonun Formation. As mineralization proceeded and filled channels, intermittent movement on the Footwall fault led to fracturing in adjoining rocks, with resultant increases in permeability for ore fluids transport.

Mineral deposition in the system followed a well-defined paragenetic sequence, with apparently sporadic abrupt decreases in temperature of the ore fluid. As deposition continued, temperatures ranged from 300°C to 130°C, as indicated by preliminary fluid inclusion geothermometry data (Shen *et al.*, 1981). Inclusion data also indicate low salinities; thus, the ore fluid is thought to have originated as pore water within the Skonun Formation. Metals are believed by the authors to have been derived from the Skonun Formation, in part by alteration of volcanic fragments and in part by dissolution of heavy minerals. It appears likely that precipitation of gold was to some extent promoted by the abundant organic material within the Skonun Formation.

Acknowledgments

The financial support of Consolidated Cinola Mines Ltd. for our study has been gratifying. In particular, the cooperation and assistance of K.G. Sanders, president, and A. MacKillop,

FIGURE 12 (facing page). Ore Mineral Associations.

A) Drillhole 77-9, 30 m: pyrite partly replaced by marcasite (Mc), with quartz and organic matter (CM, black) as the gangue minerals.
B) Drillhole 78-6, 77 m: euhedral pyrite (Py) and finely disseminated rutile (Rt) (pale grey).
C) Drillhole 79-10, 143 m: inclusions of magnetite (dark grey) and hematite (Hm) (grey) in pyrrhotite (Po) (pale grey), surrounded by pyrite (Py) (white).
D) Drillhole 77-9, 2 m: inclusions of globular pyrite (near white) in cinnabar (pale grey).
E) Drillhole 78-6, 157 m: polymineralic aggregate of pyrite (pale grey), chalcopyrite (medium grey), galena (medium grey) and sphalerite (dark grey).
F) Drillhole 78-6, 157 m: galena (Ga) (pale grey) veinlet crosscutting sphalerite (dark grey), pyrite (medium grey), chalcopyrite (medium grey) and visible gold (Gd) (white).
G) Drillhole 78-6, 173 m: gold (Gd) (white) included in chalcopyrite (pale grey), with pyrite (Py) also visible.
H) Drillhole 79-9, 26 m: quartz crystals (Qx) projecting toward the interior of a vein coated by fine-grained drusy quartz (Qx) and gold (Gd), which in turn is covered by a layer of fine-grained pyrite (Py).

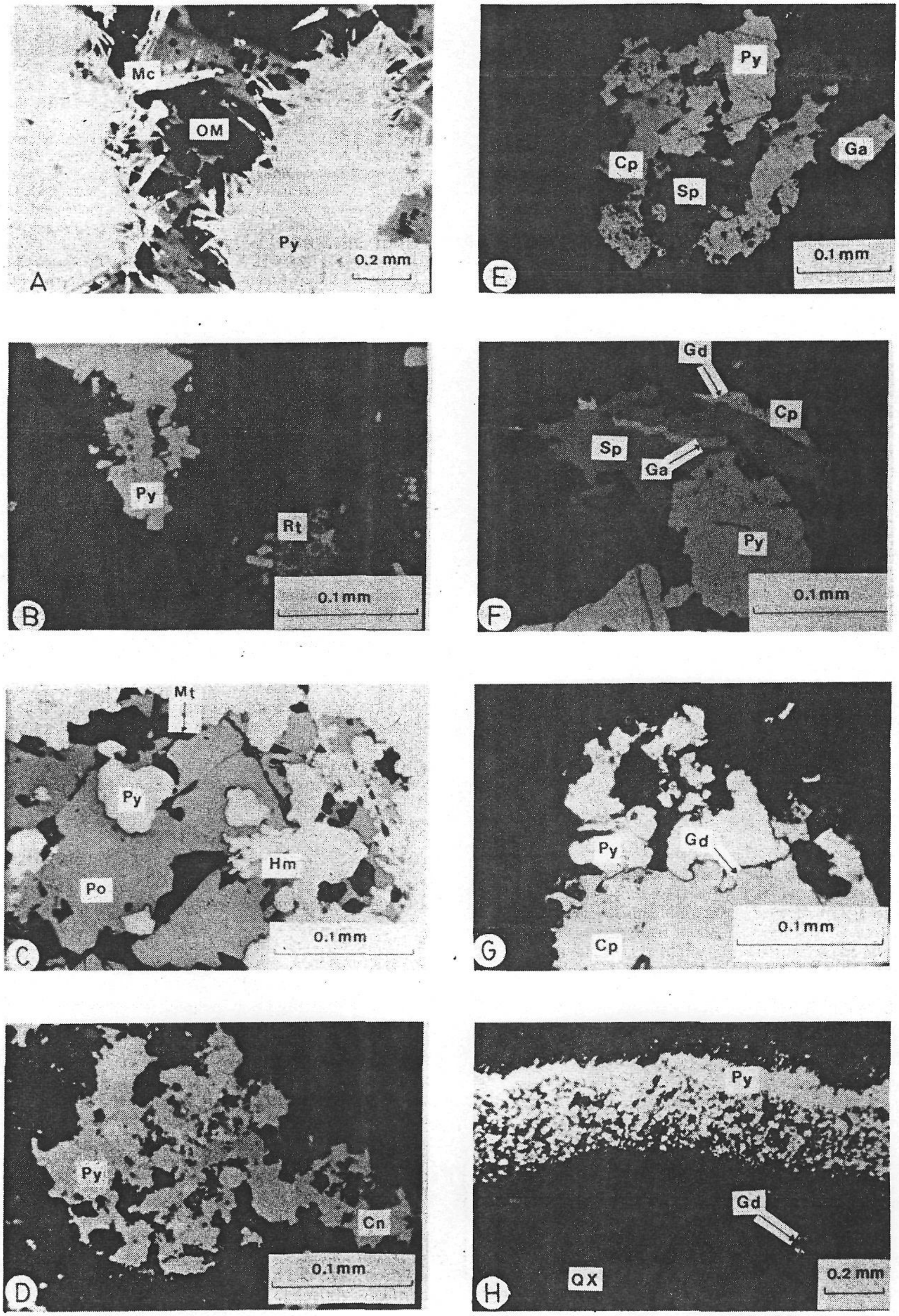
Mc
OM
Py
0.2 mm
A
Py
Ga
Cp
Sp
0.1 mm
E
Py
Rt
0.1 mm
B
Gd
Cp
Sp
Ga
Py
0.1 mm
F
Mt
Py
Hm
Po
0.1 mm
C
Py
Gd
0.1 mm
Cp
G
Py
Cn
0.1 mm
D
Py
Gd
QX
0.2 mm
H

camp manager, is acknowledged with thanks. The laboratory work was funded in part by a N.S.E.R.C. Scholarship to Champigny and a grant from the B.C. Ministry of Energy, Mines and Petroleum Resources. H.J. Mah, P.H. Blanchet and T. Chen (International Geosystems Corp.) advised on the use of the GEOLOG system. John Gardiner provided technical assistance in the field. Discussions with Dr. A. Sutherland Brown and a visit with him to the type locality of the Skonun Formation were extremely beneficial to this study.

REFERENCES

BLANCHET, P.H., and GODWIN, C.I., 1972, 'Geolog System' for computer and manual analysis of geologic data from porphyry and other deposits; *Econ. Geol., v. 67, p. 796-813.*

BLATT, H., MIDDLETON, G.V., and MURRAY, R., 1972, *Origin of Sedimentary Rocks;* Prentice-Hall Inc., Englewood Cliffs, N.J., 634 p.

CHAMPIGNY, N., and SINCLAIR, A.J., 1980, Progress report on the geology of the Specogna (Babe) gold deposit; *B.C. Ministry of Energy, Mines and Petroleum Res., Paper 1980-1, p. 158-170.*

CHAMPIGNY, N., SINCLAIR, A.J., and SANDERS, K.G., 1980, Specogna gold deposit of Consolidated Cinola Mines, an example of structured property evaluation; *Western Miner, v. 53, pp. 35-44.*

CHAMPIGNY, N., HENDERSON, C., and ROUSE, G.E., 1981, New evidence for the age of the Skonun Formation, Queen Charlotte Islands, B.C.; *Can. Jour. Earth Sciences, v. 18, n. 12, p. 1900-1903.*

GODWIN, C.I., HINDSON, R.E., and BLANCHET, P.H., 1977, GEOLOG: A computer-based scheme for detailed analysis of stratigraphy, especially as applied to data from drill holes in coal exploration or development; *CIM Bull., v. 70, n. 783, p. 123-132.*

McMILLAN, W.J., and PANTELEYEV, A., 1980, Ore Deposit Models I. Porphyry copper deposits; *Geoscience Canada, v. 7, n. 2, p. 52-63.*

MIALL, A.D., 1978, Lithofacies types and vertical profile models in braided river deposits: a summary; *in* Miall, A.D. (editor), *Can. Soc. Petroleum Geol., Memoir 5, Fluvial Sedimentology, p. 507-604.*

RICHARDS, G.G., CHRISTIE, J.S., and WOLFHARD, M.R., 1976, Specogna: a Carlin-type gold deposit, Queen Charlotte Islands, British Columbia (abstract); *CIM Bull., v. 69, n. 773, p. 64.*

RICHARDS, G.G., CHRISTIE, J.S., and LIVINGSTONE, K.W., 1979, Some gold deposits of the Queen Charlotte Islands (abstract); *CIM Bull., v. 72, n. 809, p. 64.*

RUST, B.R., 1972, Structure and process in a braided river; *Sedimentology, v. 18, p. 221-246.*

RUST, B.R., 1978, Depositional models for braided alluvium; *in* Miall, A.D. (editor), *Can. Soc. Petroleum Geol., Memoir 5, Fluvial Sedimentology, pp. 605-625.*

SHEN, K., CHAMPIGNY, N., and SINCLAIR, A.J., 1981, Genetic implications of fluid inclusion studies, Cinola gold deposit, Queen Charlotte Islands, B.C.; *B.C. Ministry of Mines and Pet. Res., Paper 1981-1, p. 197-200.*

SUTHERLAND BROWN, A., 1968, Geology of the Queen Charlotte Islands, British Columbia; *B.C. Ministry of Energy, Mines & Pet. Res., Bull. 54.*

SUTHERLAND BROWN, A., and SCHROETER, T.G., 1975, Report on the Babe gold prospect, Queen Charlotte Islands; *B.C. Ministry of Energy, Mines & Pet. Res., Geological Fieldwork, 1975, p. 71-75.*

SUTHERLAND BROWN, A., and SCHROETER, T.G., 1977, Babe gold prospect; *B.C. Ministry of Energy, Mines and Pet. Res., Geology in B.C., 1975, p. G73-G77.*

TAYLOR, R.P., and FRYER, B.J., 1980, Multiple stage hydrothermal alteration in porphyry copper systems in northern Turkey: the temporal interplay of potassic, propylitic and phyllic fluids; *Can. J. Earth Sc., v. 17, n. 7, p. 901-926.*

VONDRA, C.F., and BURGGRAF, D.R., Jr., 1978, Fluvial facies of the Plio-Pleistocene Kooli Fora Formation, Karari Ridge, East Lake Turkana, Kenya; *in* Miall, A.D. (editor), *Can. Soc. Petroleum Geol., Memoir 5, Fluvial sedimentology, p. 511-529.*

YOUNG, I.F., and CHASE, R.L., 1976, Gravity and seismic profiles over the Sandspit Fault, Queen Charlotte Islands, B.C.; *B.C. Dept. of Mines and Pet. Res., Geological Fieldwork, 1976, p. 59-64.*